Multibunch instabilities studies at Diamond

R. Bartolini

Diamond Light Source
and
John Adams Institute, University of Oxford

thanks: R. Fielder, S. Pande, G. Rehm, V. Smalyuk (BNL)

TWIICE - II
Abingdon, 9 February 2016

Outline

- (Short) review of main results of the theory of multi-bunch instability
- Data from Diamond TMBF system
- Impedance analysis and comparison with CST simulations **(WIP)**
- Open issues

Transverse multibunch oscillations - no wakefields

Each bunch oscillates with the betatron frequency $\omega_{x,y}$

In a multi-bunch train without wakefields all bunches are independent

The motion can be expanded in Fourier modes, (M bunches = M modes, and in full fill, M = harmonic number)

However, without wakefields there is no reason to prefer this set to any other "basis"

(i.e. modes are degenerate)

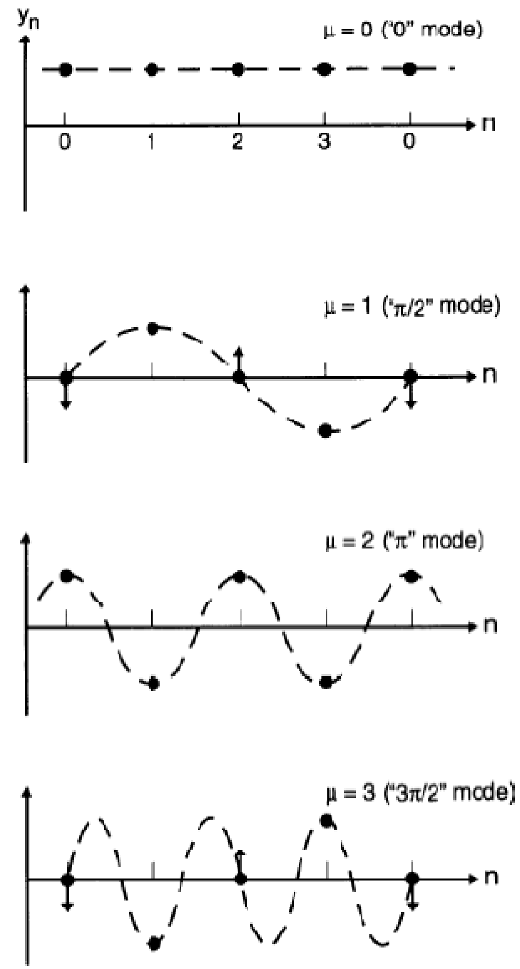

Multibunch oscillations - with transverse wakefields

Bunches are now coupled by the wakefields

Each bunch oscillates with the betatron frequency $\Omega_{x,y}$

In the limit of small wakefields (linear wakes) the Fourier modes are eigenvectors of the time evolution, i.e. modes are preserved during the time evolution

$$\psi_n(r,\phi,s) = \psi_0(r) + \psi_1(r,\phi)\exp\left[-i\Omega\left(\frac{s}{c} - \frac{nT_0}{M}\right)\right]\exp\left(2\pi i\frac{\mu n}{M}\right),$$

$$n = 0, 1, \ldots, M-1, \quad (6.233)$$

The betatron oscillation frequency becomes complex

Im$\Omega \Rightarrow$ damping or anti-damping
Re$\Omega \Rightarrow$ frequency shift

The degeneracy of the Fourier modes is broken, i.e. $\Omega = \Omega(\mu)$

Complex frequency shift and driving impedance

For zero length (point-like) bunches (see e.g. A. Chao)

$$\Omega^{(\mu)} - \omega_\beta = -i\frac{MNr_0\,c}{2\gamma T_0^2\omega_\beta}\sum_{p=-\infty}^{\infty} Z_1^{\perp}[(pM+\mu)\omega_0+\omega_\beta]$$

e.g.

$$\mathrm{Re}\,\Omega^{(\mu)} = \omega_\beta + \frac{MNr_0\,c}{2\gamma T_0^2\omega_\beta}\,\mathrm{Im}\sum_{p=-\infty}^{\infty} Z_1^{\perp}[(pM+\mu)\omega_0+\omega_\beta]$$

coherent tuneshift
(ReΩ = ImZ)

$$\mathrm{Im}\,\Omega^{(\mu)} = -\frac{MNr_0\,c}{2\gamma T_0^2\omega_\beta}\,\mathrm{Re}\sum_{p=-\infty}^{\infty} Z_1^{\perp}[(pM+\mu)\omega_0+\omega_\beta]$$

growth rate
(Im Ω = ReZ)

mode μ is driven by the impedance computed at $(pM + \mu)\omega_0 + \omega_\beta$

Complex frequency shift and driving impedance

For Gaussian rigid bunches with rms bunch duration σ_τ

$$\Omega^{(\mu)} - \omega_\beta = -i\frac{MNr_0\,c}{2\gamma T_0^2\omega_\beta}\sum_{p=-\infty}^{\infty} Z_1^\perp[(pM+\mu)\omega_0 + \omega_\beta]\cdot e^{-[(pM+\mu)\omega_0+\omega_\beta]^2\sigma_\tau^2}$$

e.g.

$$\mathrm{Re}\,\Omega^{(\mu)} = \omega_\beta + \frac{MNr_0\,c}{2\gamma T_0^2\omega_\beta}\,\mathrm{Im}\sum_{p=-\infty}^{\infty} Z_1^\perp[(pM+\mu)\omega_0 + \omega_\beta]\cdot e^{-[(pM+\mu)\omega_0+\omega_\beta]^2\sigma_\tau^2}$$

coherent tuneshift
($\mathrm{Re}\Omega$ = ImZ)

$$\mathrm{Im}\,\Omega^{(\mu)} = -\frac{MNr_0\,c}{2\gamma T_0^2\omega_\beta}\,\mathrm{Re}\sum_{p=-\infty}^{\infty} Z_1^\perp[(pM+\mu)\omega_0 + \omega_\beta]\cdot e^{-[(pM+\mu)\omega_0+\omega_\beta]^2\sigma_\tau^2}$$

growth rate
(Im Ω = ReZ)

mode μ is driven by the impedance computed at $(pM + \mu)\omega_0 + \omega_\beta$

Non rigid bunches

For bunches with finite length – and internal modes (see e.g. A. Chao)

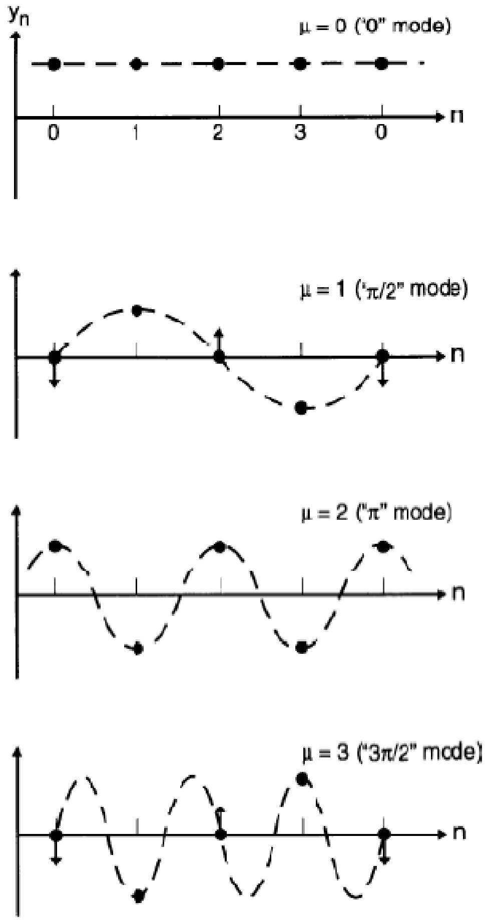

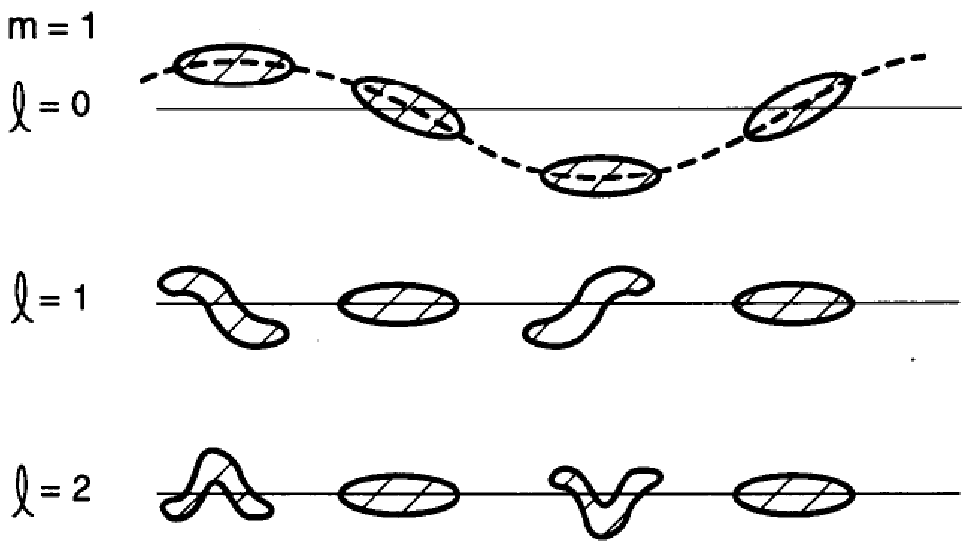

Complex frequency shift and driving Impedance

For bunches with finite length – and internal modes (see e.g. A. Chao)

$$\Omega^{(\mu,l)} - \omega_\beta = -i\frac{MNr_0\,c}{2\gamma T_0^2\omega_\beta}\sum_{p=-\infty}^{\infty} Z_1^{\perp}[(pM+\mu)\omega_0 + \omega_\beta + l\omega_s]\cdot\rho_l[(pM+\mu)\omega_0 + \omega_\beta + l\omega_s]$$

e.g.

coherent tuneshift (ReΩ = ImZ)

$$\mathrm{Re}\,\Omega^{(\mu,l)} = \omega_\beta + \mathrm{Im}\frac{MNr_0\,c}{2\gamma T_0^2\omega_\beta}\sum_{p=-\infty}^{\infty} Z_1^{\perp}[(pM+\mu)\omega_0 + \omega_\beta + l\omega_s]\cdot\rho_l[(pM+\mu)\omega_0 + \omega_\beta + l\omega_s]$$

growth rate (Im Ω = ReZ)

$$\mathrm{Im}\,\Omega^{(\mu,l)} = -\mathrm{Re}\frac{MNr_0\,c}{2\gamma T_0^2\omega_\beta}\sum_{p=-\infty}^{\infty} Z_1^{\perp}[(pM+\mu)\omega_0 + \omega_\beta + l\omega_s]\cdot\rho_l[(pM+\mu)\omega_0 + \omega_\beta + l\omega_s]$$

mode (μ, l) is driven by the impedance computed at $(pM + \mu)\omega_0 + \omega_\beta + l\omega_s$

Complex frequency shift and driving Impedance

With non-zero chromaticity the bunch frequency spectrum is shifted by

$\omega_\xi = \xi\omega_\beta/\eta$ and naming $\omega_{\mu,l} = (pM + \mu)\omega_0 + \omega_\beta + l\omega_s$

e.g.

$$\Omega^{(\mu,l)} - \omega_\beta = -i\frac{MNr_0 c}{2\gamma T_0^2\omega_\beta}\sum_{p=-\infty}^{\infty} Z_1^\perp(\omega_{\mu,l})\cdot\rho_l(\omega_{\mu,l}-\omega_\xi)$$

$$\Omega^{(\mu,l)} = \omega_\beta + \mathrm{Im}\frac{MNr_0 c}{2\gamma T_0^2\omega_\beta}\sum_{p=-\infty}^{\infty} Z_1^\perp(\omega_{\mu,l})\cdot\rho_l(\omega_{\mu,l}-\omega_\xi)$$

coherent tuneshift ($\mathrm{Re}\Omega$ = ImZ)

$$\Omega^{(\mu,l)} = -\mathrm{Re}\frac{MNr_0 c}{2\gamma T_0^2\omega_\beta}\sum_{p=-\infty}^{\infty} Z_1^\perp(\omega_{\mu,l})\cdot\rho_l(\omega_{\mu,l}-\omega_\xi)$$

growth rate (Im Ω = ReZ)

The bunch samples the impedance at $\omega_{\mu,l}$ but the bunch frequency spectrum is shifted at $\omega_{\mu,l} - \omega_\xi$

Sampling in time and aliasing in frequency

A mode μ sampled turn-by-turn corresponds to the frequency

$\mathrm{frac}(\Omega_{x,y})$ aliased in $[0, \omega_0] \rightarrow \mathrm{frac}(\Omega_{x,y})$
i.e. fractional part of the tune

A mode μ sampled bunch-by-bunch corresponds to the frequency

$\mu\omega_0 + \Omega_{x,y}$ aliased in $[0, M\omega_0] \rightarrow$ i.e. baseband of the RF

For real signal the spectrum is further folded symmetrically in $[0 , M\omega_0/2]$

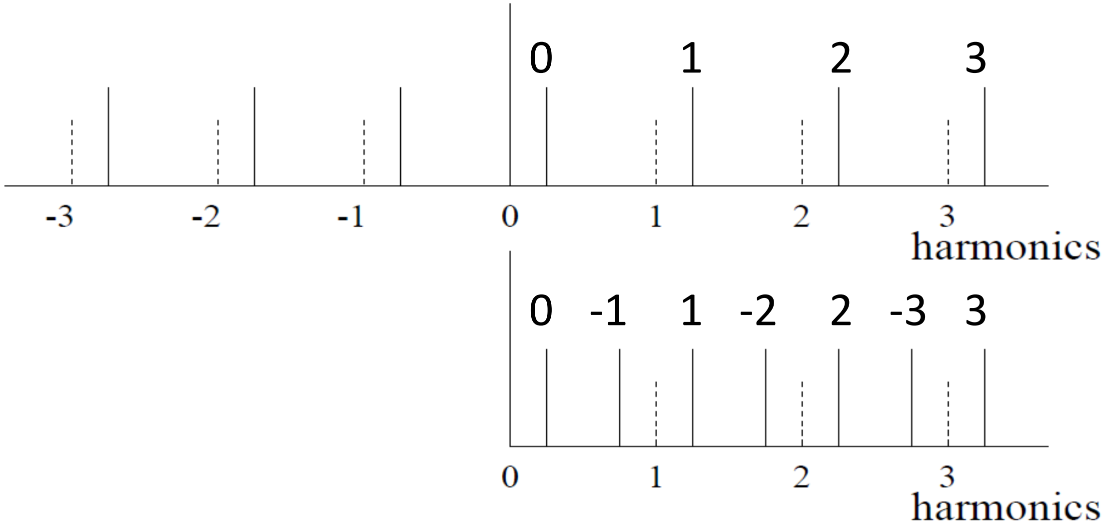

Modes $\mu = 0 , 1, , ..., M - 1$

Modes $\mu = 0 , 1, , ..., M - 1$ folded, i.e.

$- 1 = M - 1$

$- 2 = M - 2$

...

Grow damp experiment

1)
Artificially excite mode μ by using a stripline driven at the frequency

$$(pM + \mu)\omega_0 + \omega_\beta$$

2)
Stop the excitation and measure free oscillations (damped or anti damped)

3)
Run feedback to damp any unstable mode or any residual oscillation

Repeat for all modes $\mu = 0, 1, ..., M - 1$

Grow damp experiment at Diamond

936 bunches - 2 ns (500 MHz) – full fill M = 936
530 kHz revolution frequency –
Current up to 300 mA; bunch length 15-25 ps rms – with current

1)
Artificially excite mode μ for e.g. 250 turns at the frequency $(pM + \mu)\omega_0 + \omega_\beta$
p is optimised on the specific stripline design and operating frequency (at Diamond p = 0 corresponding to 0 – 250 MHz band)
2)
Stop the excitation and measure free oscillations for 250 turns

transfer data ***

very slow to transfer fast all bunch-by-bunch turn-by-turn data

only the Fourier component (amplitude and phase) at the frequency of interest for mode μ is stored
3)
Run feedback to damp any unstable mode or any residual oscillation for 250 turns

Grow damp experiment at Diamond

Example of mode that is naturally damped: recording the complex amplitude on a turn-by-turn basis only of the mode previously excited
Data reduced from 1.3 GB to 5.6 MB (see G. Rehm et al IBIC14)

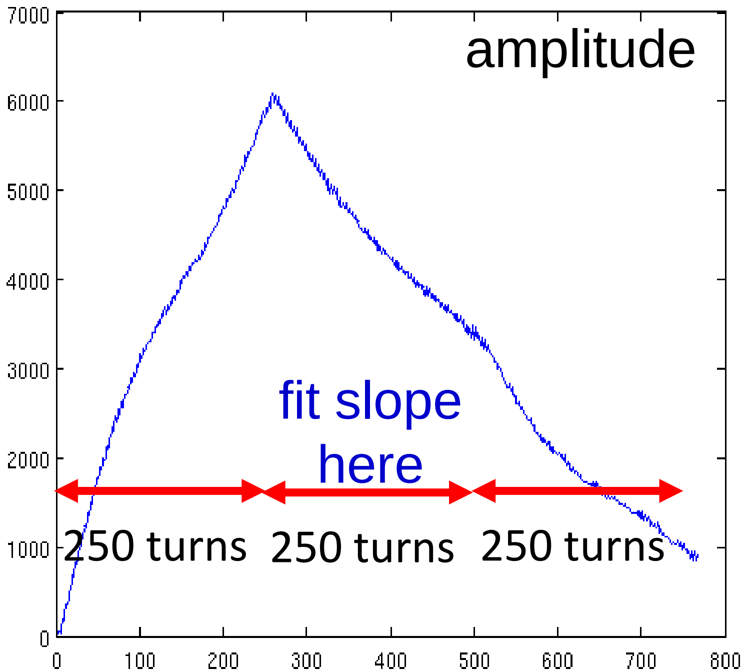

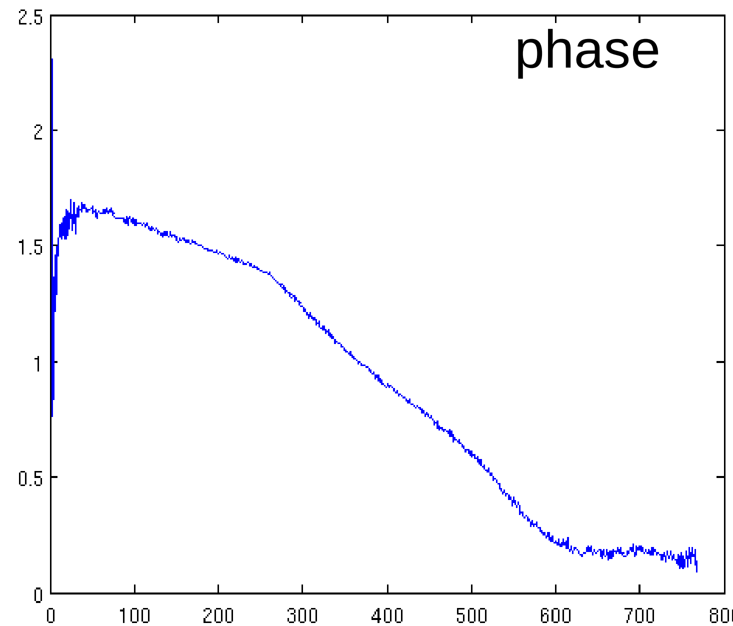

Repeat for all modes $\mu = 0, 1, \ldots, M-1$

Offline post processing gives the frequency shift and damping or growth rate (take away radiation damping and chromatic damping (if any))

Growth rates of vertical coupled bunch modes

Vertical TMF data
full fill – zero chromaticity – ID gap open
Radiation damping subtracted
blu measured – red fit

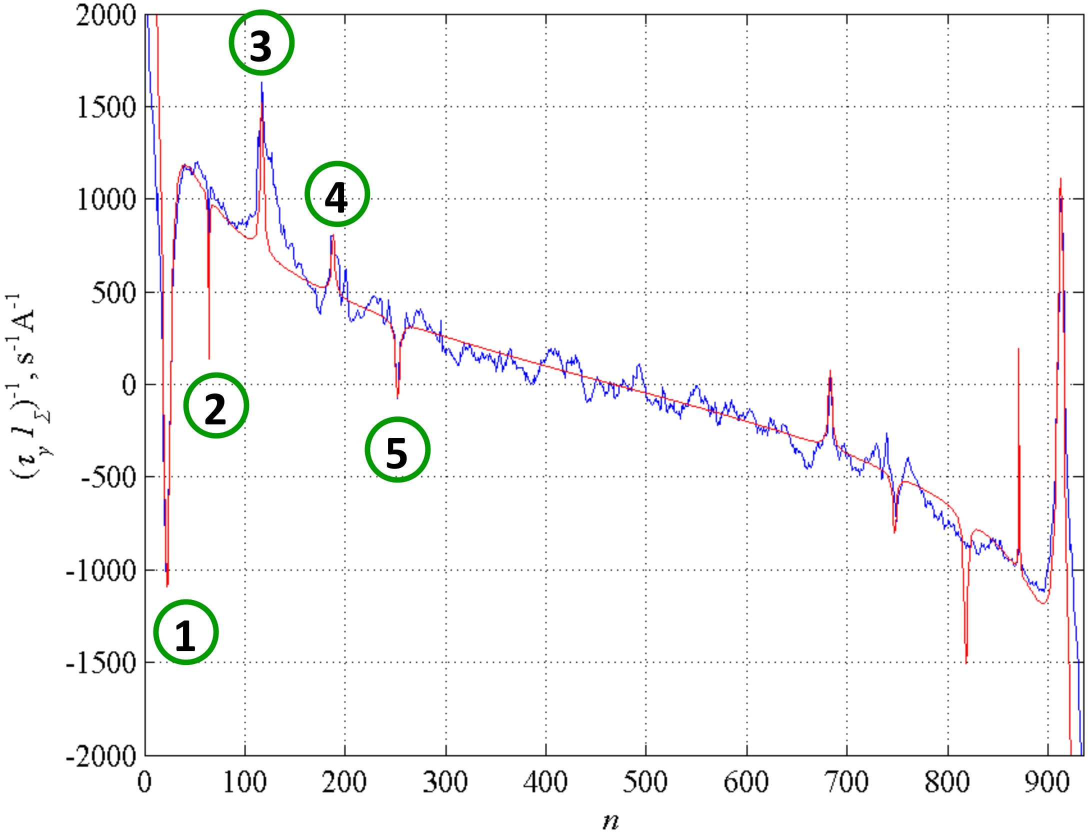

data suggest resistive wall and few high Q resonators

$$\Delta\Omega_n = -\frac{i}{4\pi}\frac{\omega_0\bar{\beta}}{E/e} I \sum_{p=-\infty}^{\infty} Z_\perp(\omega_{pn})h(\omega_{pn})$$

$$\omega_{pn} = (pN_b + n + \nu_\beta)\omega_0 \qquad h(\omega) = e^{-\omega^2\sigma^2}$$

$$Z_\perp = Z_\perp^{rw} + \sum Z_\perp^{res}$$

Resistive Wall

$\beta = 12.25$ m, $b = 13.5$ mm,
$\rho = 7.3 \cdot 10^{-7}\ \Omega\cdot$m

$$\frac{Z_{x,y}^{rw}}{L} = G_{1x,y}\frac{\operatorname{sgn}\omega + i}{\pi b^3}\sqrt{\frac{Z_0 c\rho}{2}}|\omega|^{-1/2}$$

Resonator

$$Z_\perp^{res} = \frac{R_s}{\frac{\omega}{\omega_r} + iQ\left(\frac{\omega^2}{\omega_r^2} - 1\right)}$$

Search for resonator-like structures

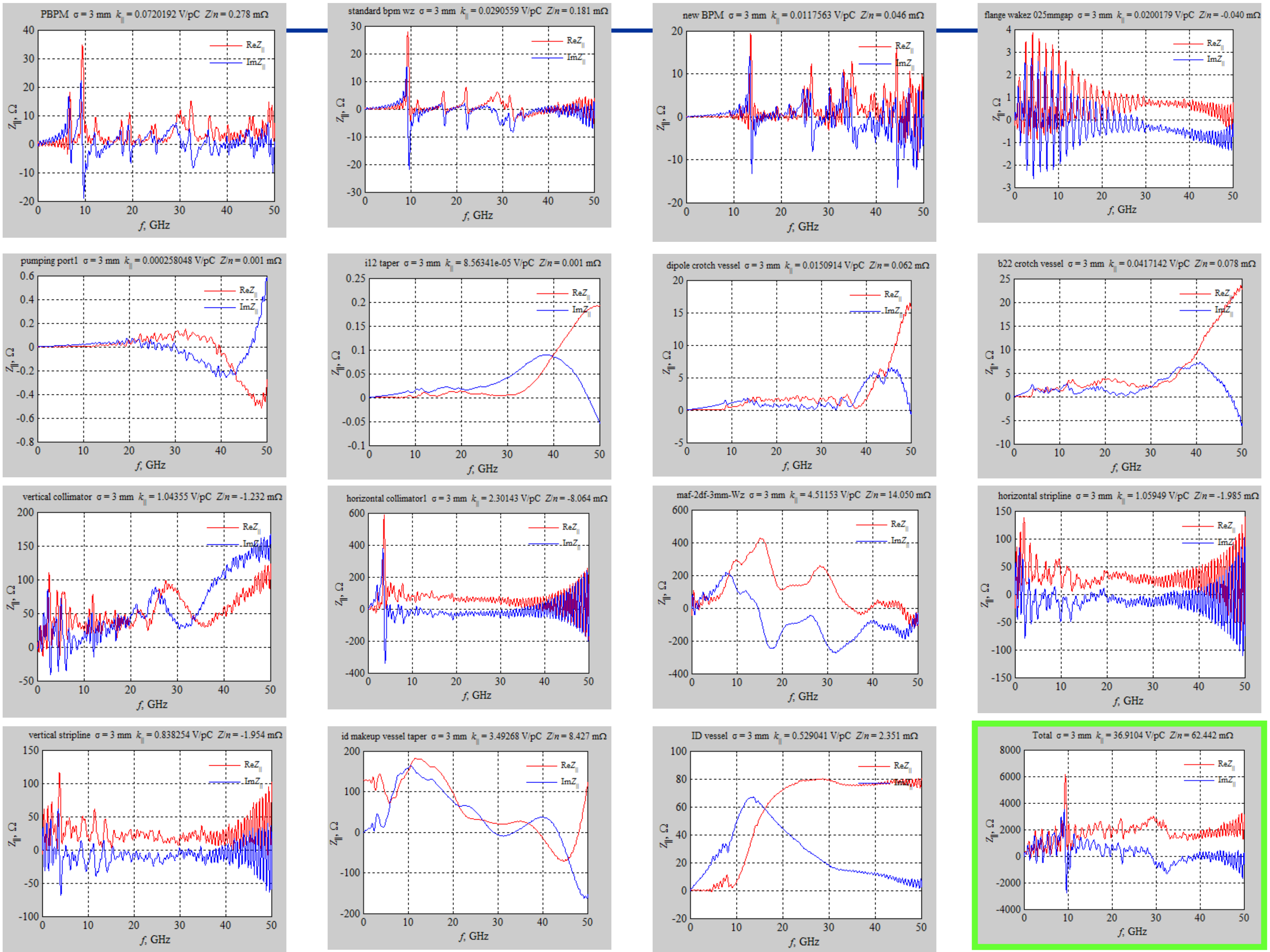

BPM buttons and enclosure

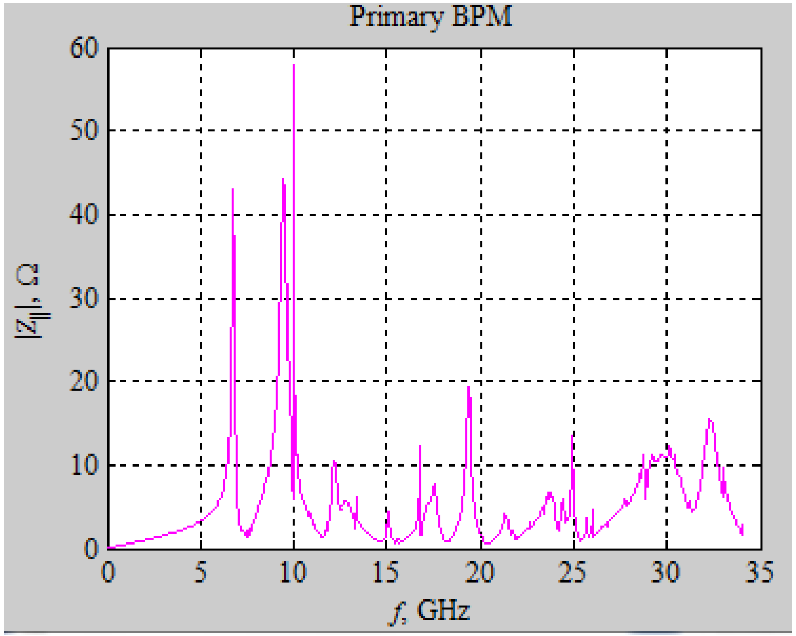

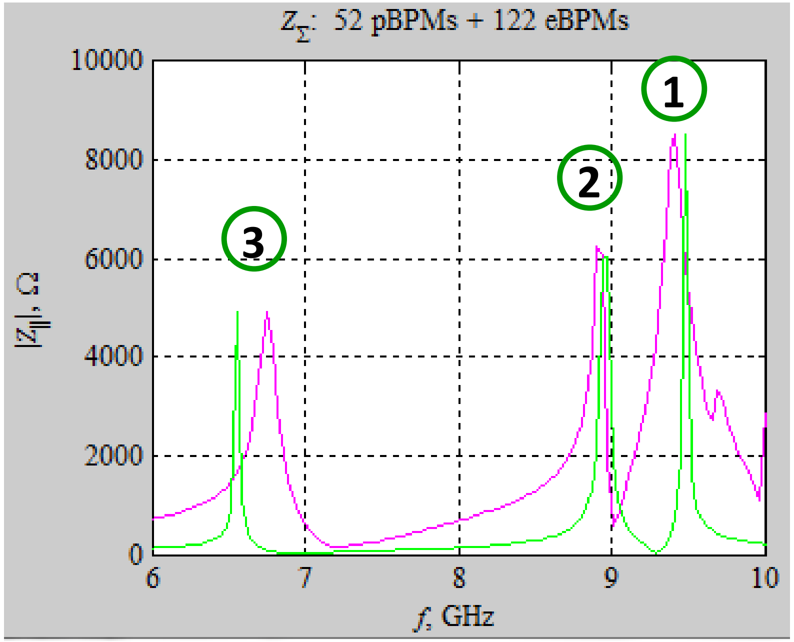

Resonance 1

$f_r = (19N_b - 22)f_0 = 9.4817$ GHz

$R_s = 2.8$ MΩ/m $Q = 2000$

Resonance 2

$f_r = (18N_b - 64)f_0 = 8.9595$ GHz

$R_s = 1.4$ MΩ/m $Q = 20000$

Resonance 3

$f_r = (13N_b + 119)f_0 = 6.5590$ GHz

$R_s = 0.8$ MΩ/m $Q = 1000$

Resonance 1 – mode -22

$f_r = 9.4200$ GHz; $Q = 2000$; $\Delta f = 61.7$ MHz

Resonance 2 – mode -64

$f_r = 8.9081$ GHz; $Q = 20000$; $\Delta f = 51.4$ MHz

Resonance 3 – mode 119

$f_r = 6.7578$ GHz; $Q = 1000$; $\Delta f = 198.8$ MHz

Effect of closing the IDs

Closing the gap of all IDs changes the geometric and RW impedance

Vertical coupled bunch modes

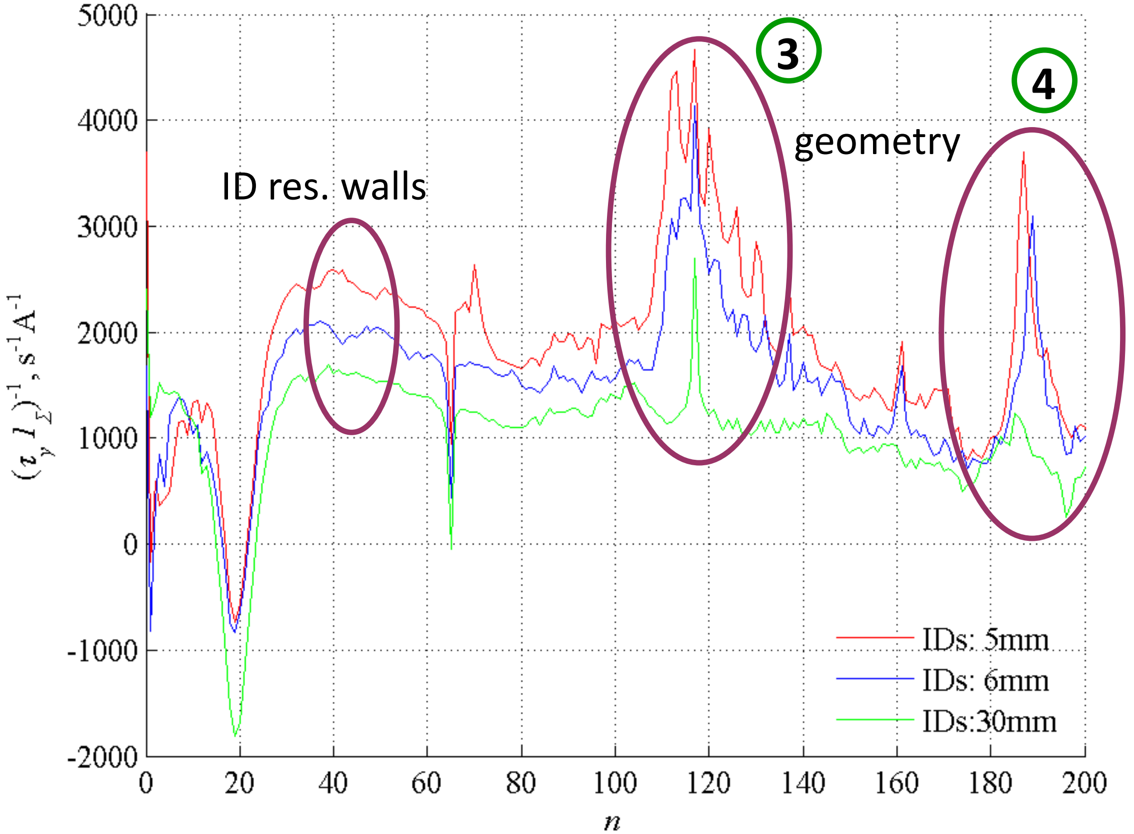

Forest of spikes at modes 100-140 has been associated to IDs

First tentative interpretation of IDs

ID gap – I04
Phase I - in vacuum ID

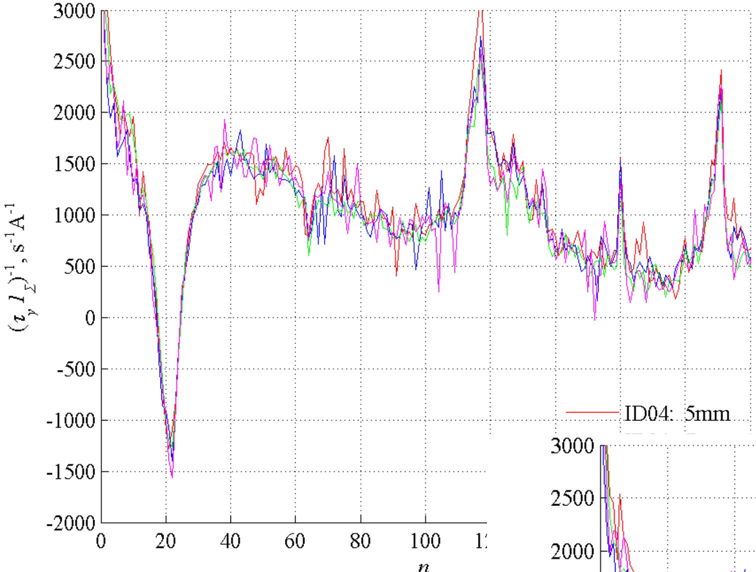

ID gap – I07: CPMU
different vessel enclosure

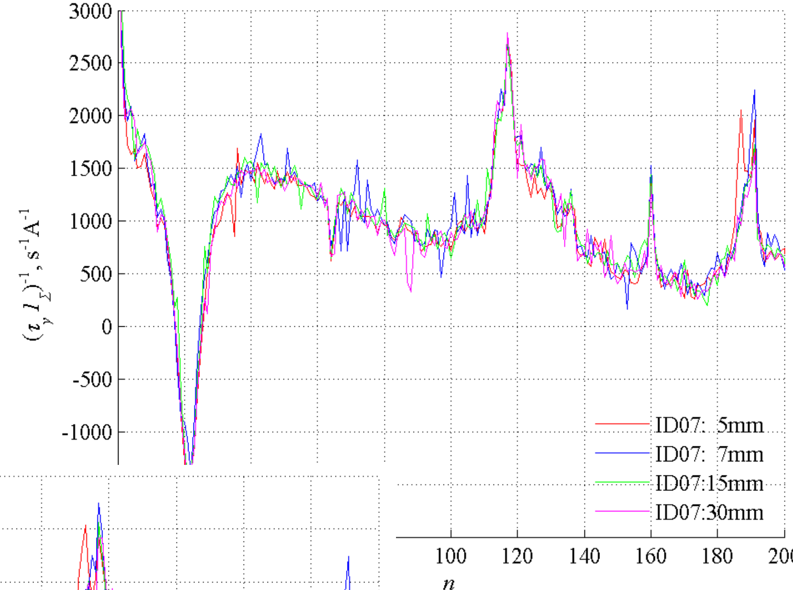

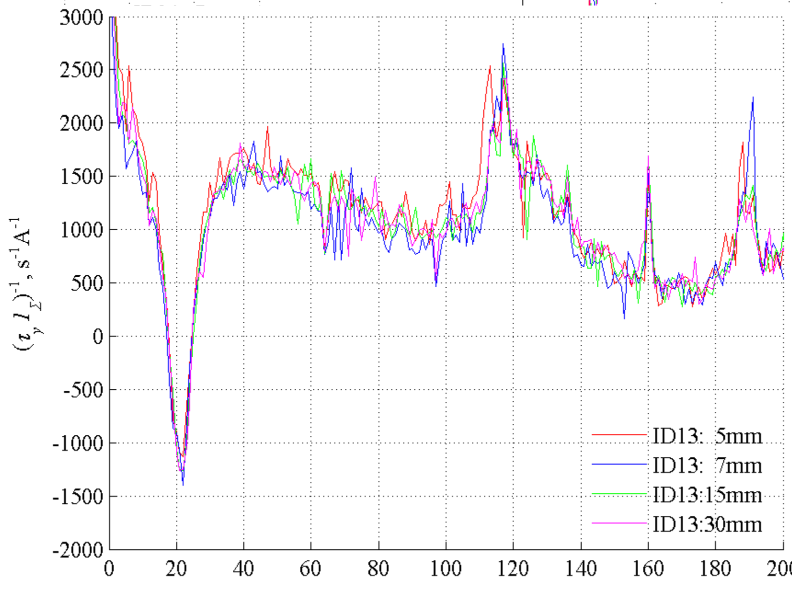

ID gap – I13:
In vacuum ID

More recent measurements

Large resonant peak moved in the last months from n = 22 now at n = 81, e.g.

Same conditions 150 mA – full fill 936 bunches – 0 chromaticity – IDs open

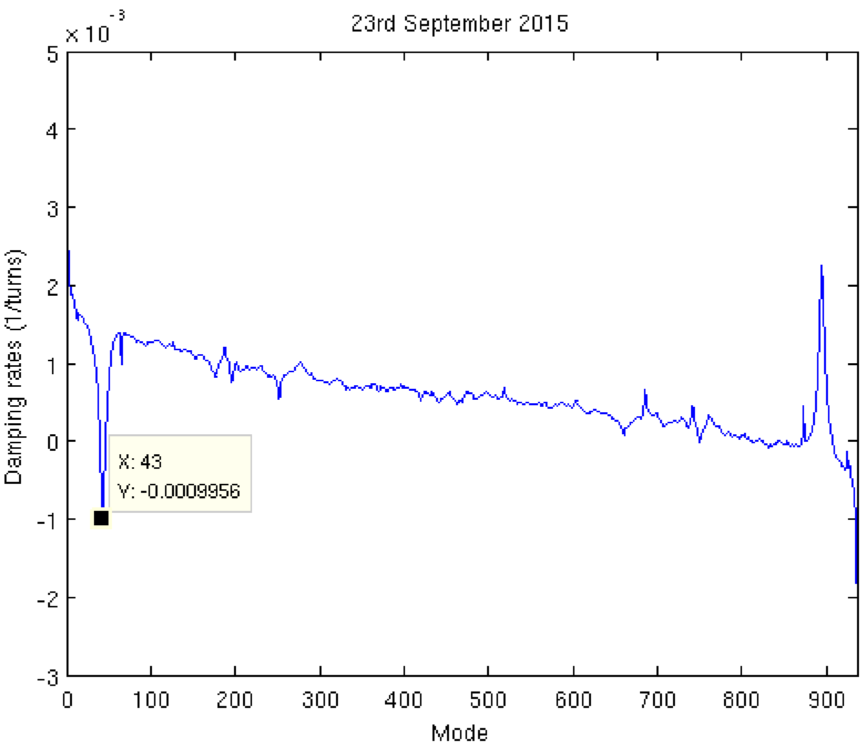

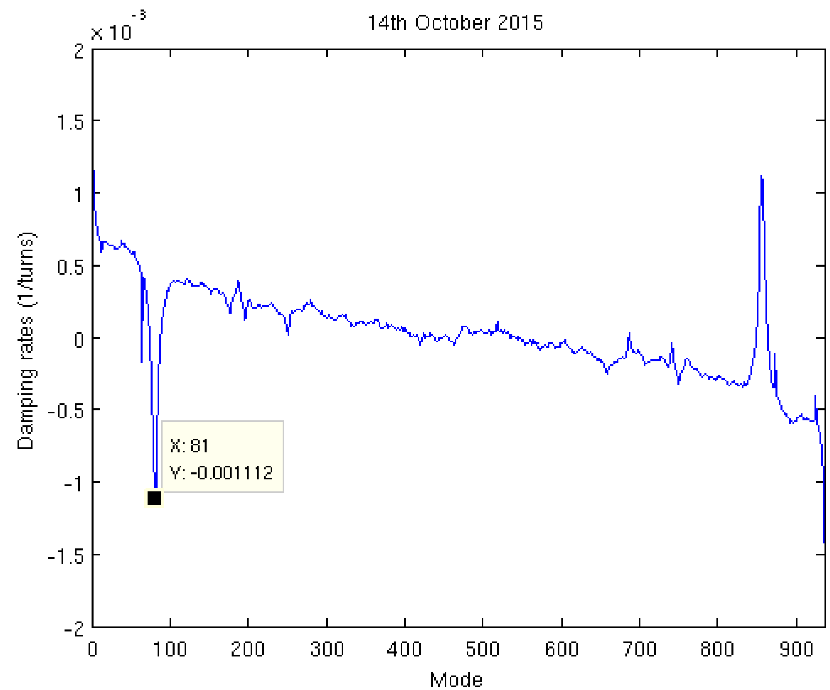

Other peaks (e.g. n = 61) are reproducible through the measurements

Investigating causes:

unlikely from BPM buttons and enclosures, other sources?

shutdown interventions? septum move; RF cavity swap

Further Machine Studies (Dec 2015)

Further machine studies revealed that the vertical collimator is responsible for the large peak in the vertical impedance (gap from 10 mm to 5.5 mm)

The peak of V impedance scans ~300 modes i.e. ~150 MHz

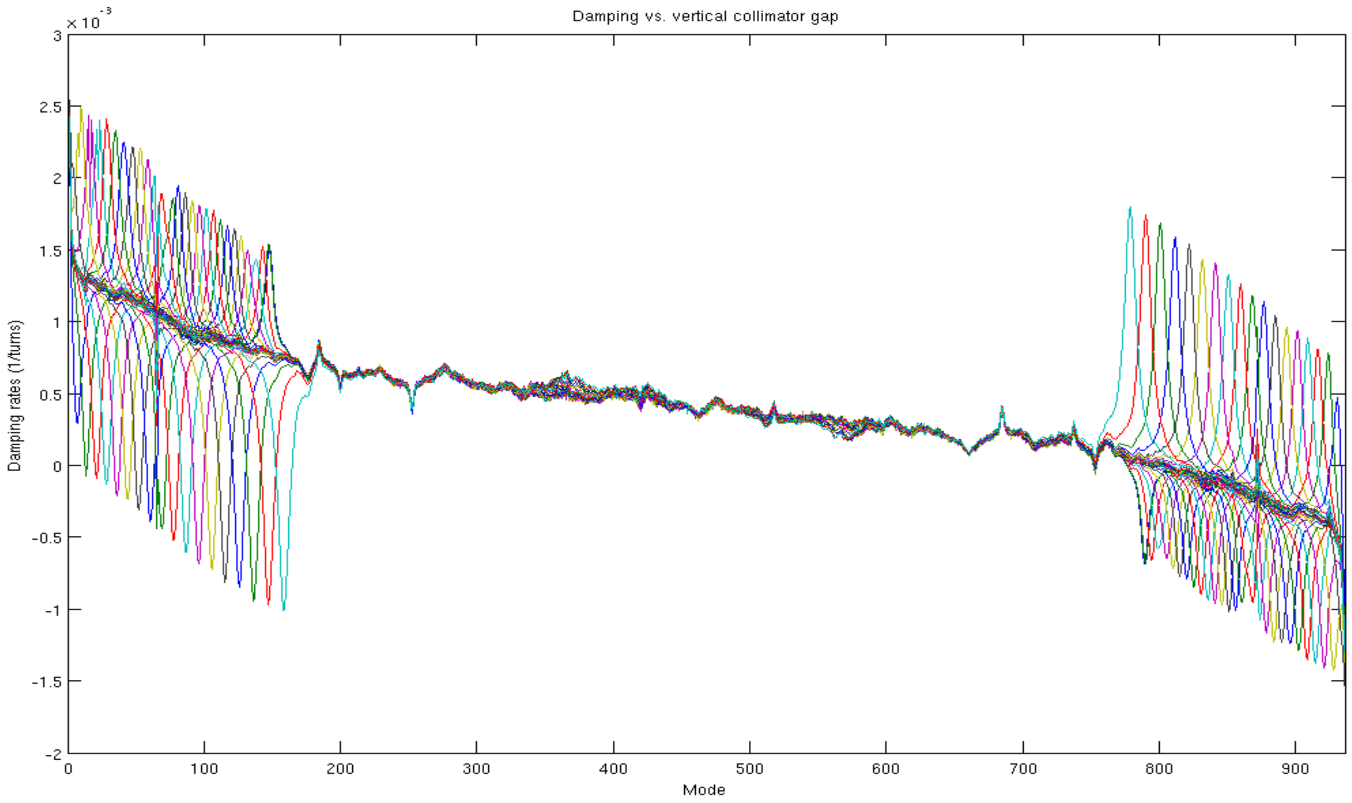

Further Machine Studies (Dec 2015)

Further machine studies revealed that the vertical collimator is responsible for the large peak in the vertical impedance (gap from 10 mm to 5.5 mm)

The peak of V impedance scans ~300 modes i.e. ~150 MHz

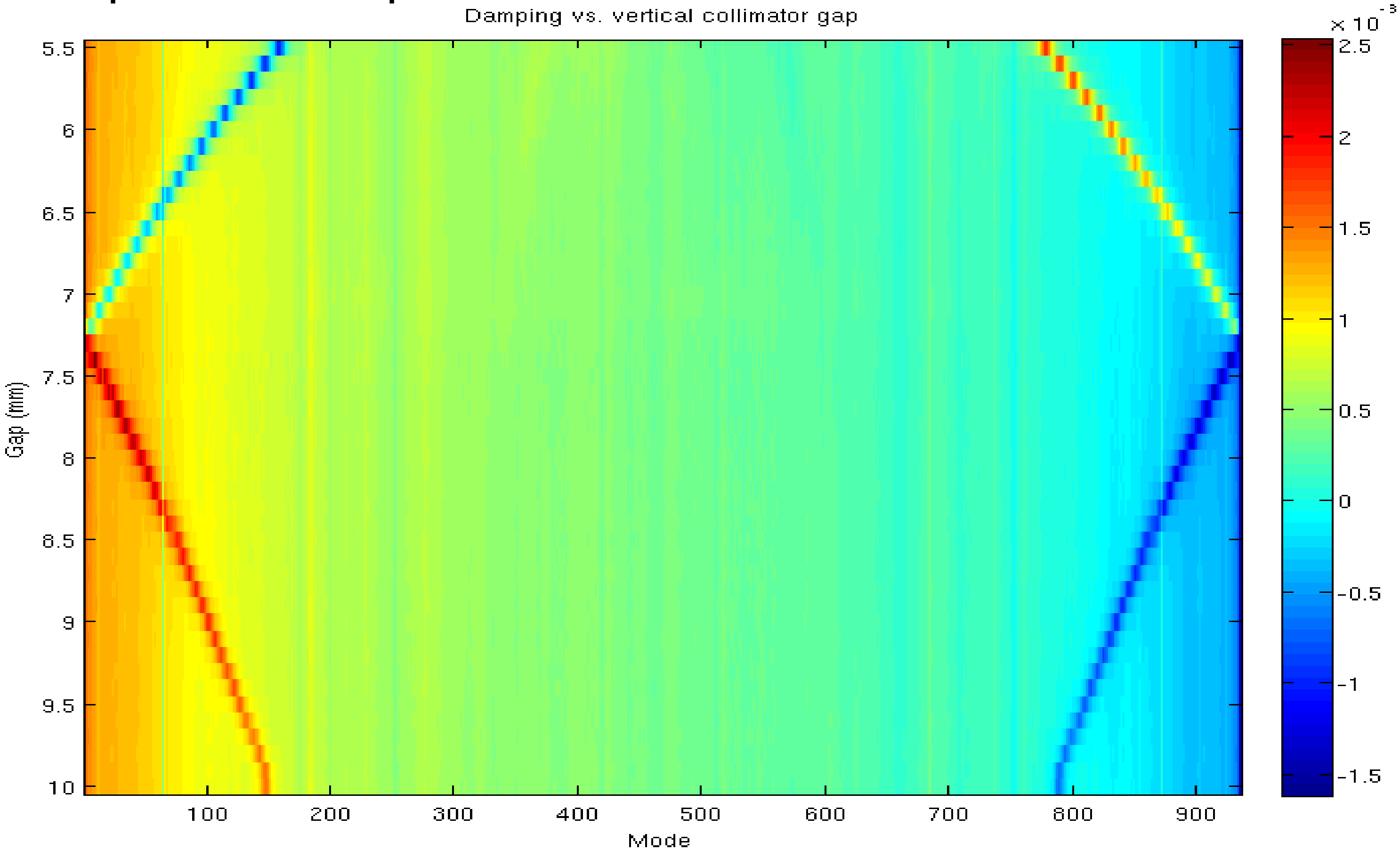

Further modelisation of collimator (I)

The failure to predict this large impedance contributor triggered a new analysis in trying to understand what features of the collimator are responsible and what level of detail should be included in the model

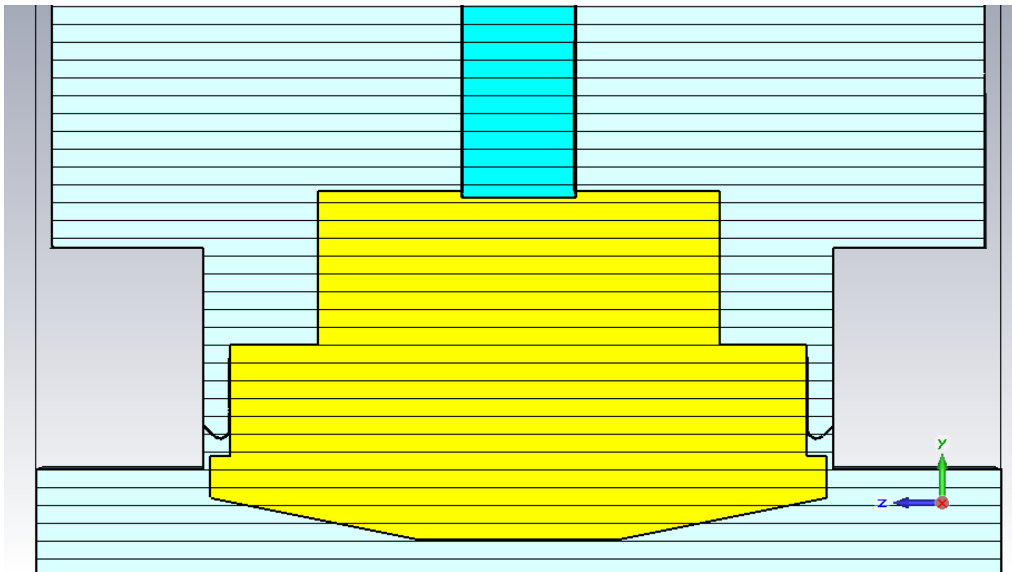

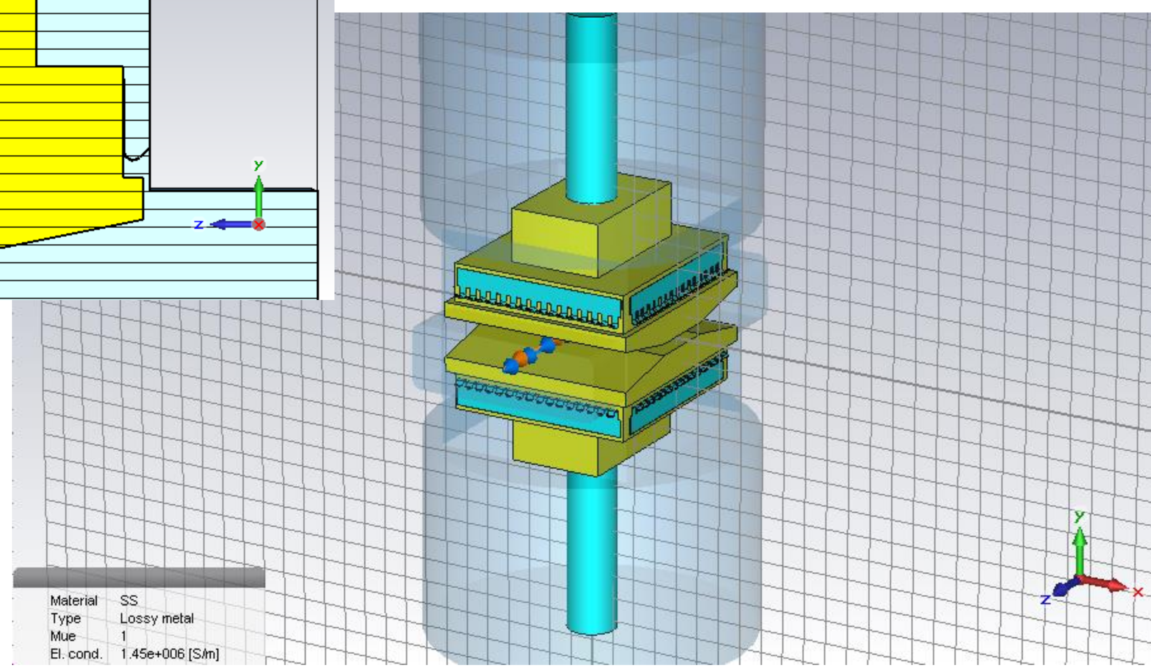

Further modelisation of collimator (II)

Vertical impedance of symmetric (top-bottom) structure
tiny shift frequency with gap (20 mm to 5 mm)

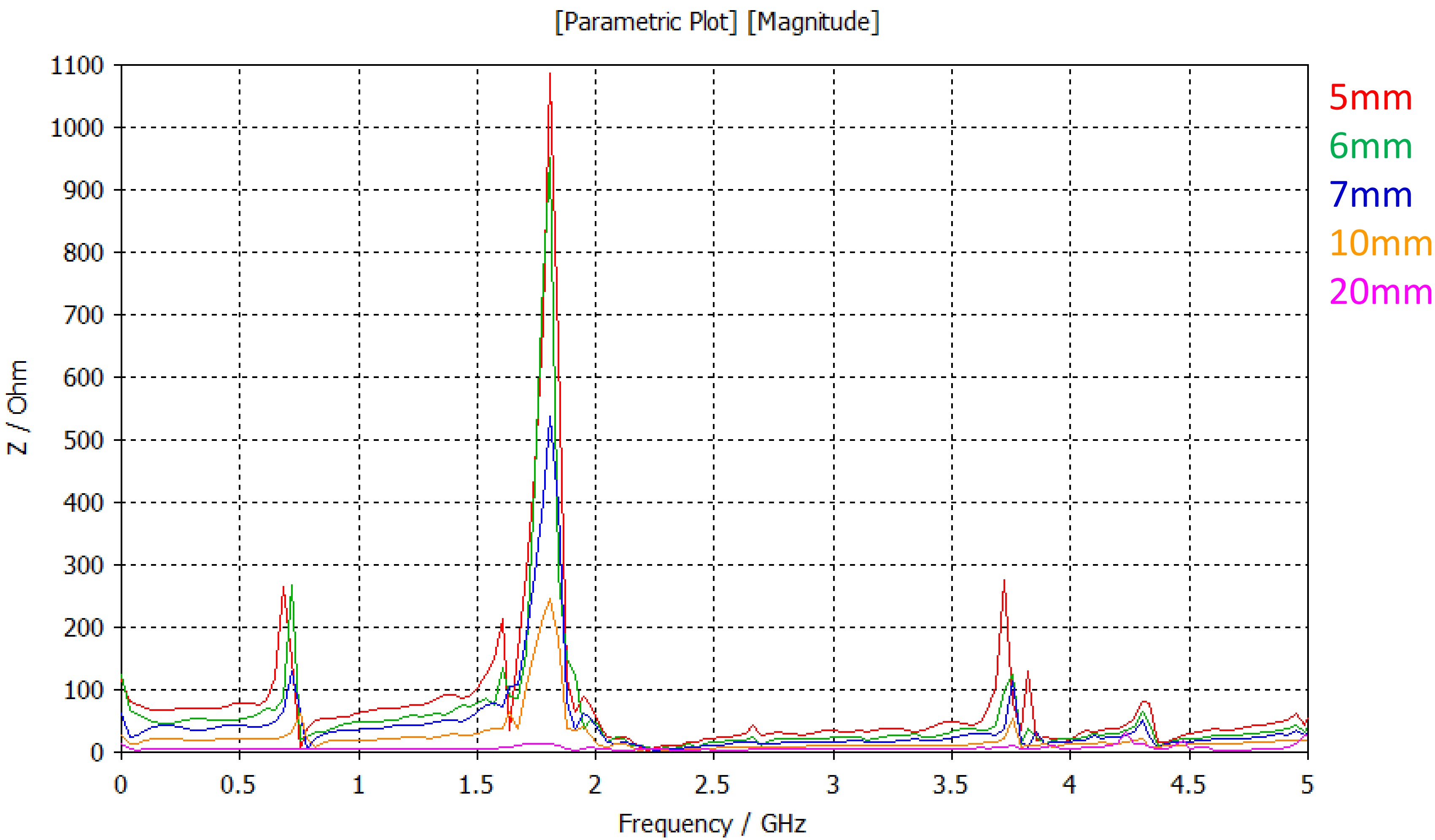

Further modelisation of collimator (III)

Trying breaking the top bottom symmetry seems to help. In in particular a broken finger…

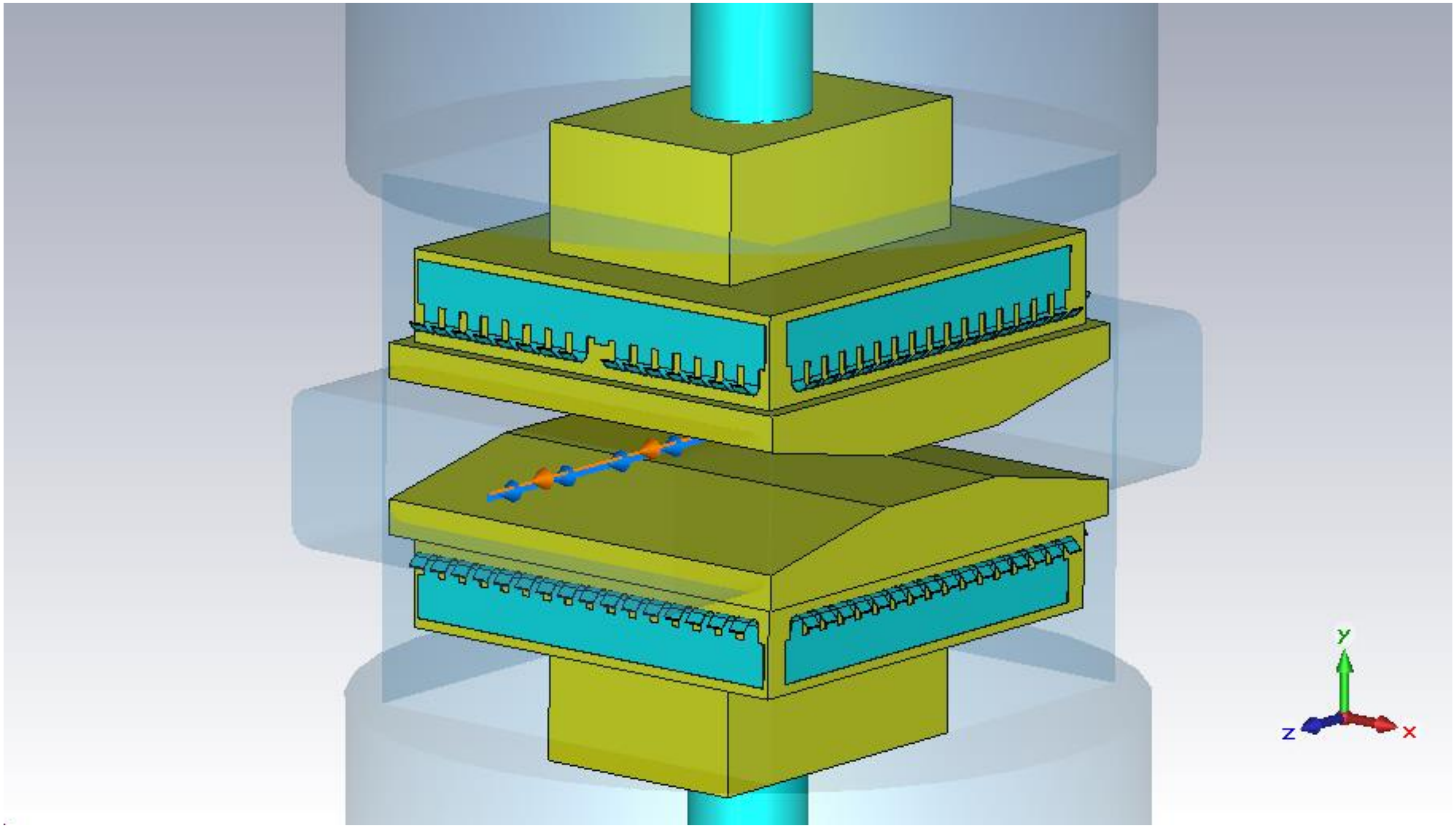

Further modelisation of collimator (IV)

in particular a broken finger generates a larger frequency shift with gap in better agreement with the one measured

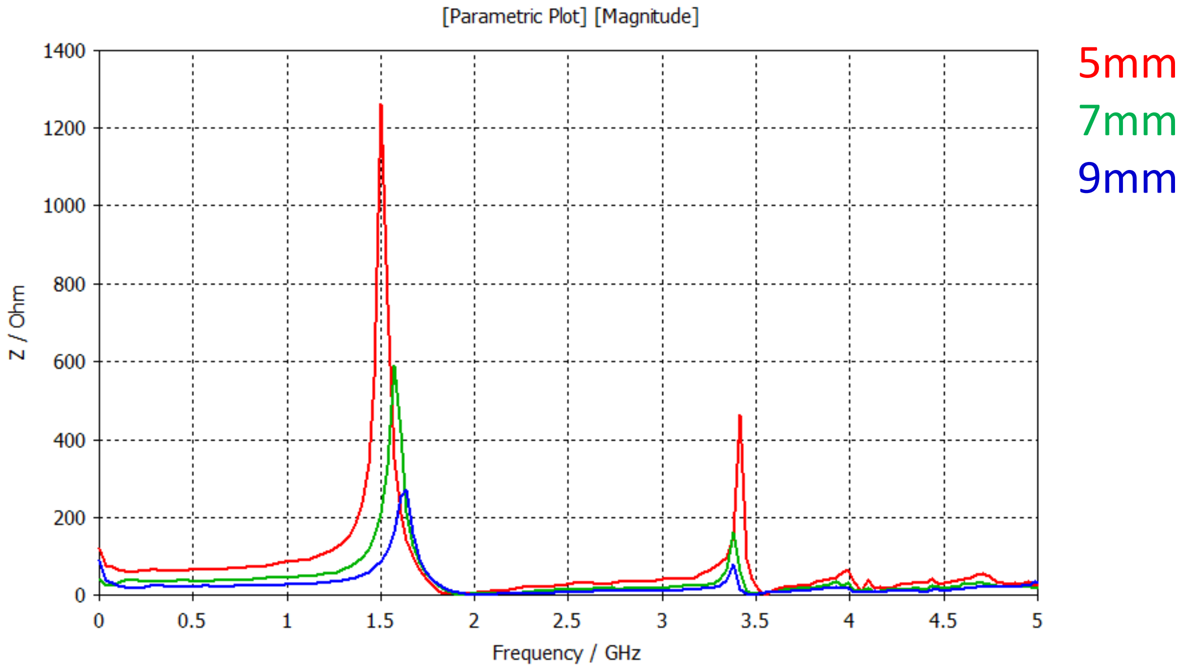

$$\Delta\Omega_n = -\frac{i}{4\pi}\frac{\omega_0\overline{\beta}}{E/e} I \sum_{p=-\infty}^{\infty} Z_\perp\left[(pN_b + n + \nu_\beta)\omega_0\right]$$

n=22:	*n*=43:	*n*=81:
f_r= 0.5116 GHz	f_r= 0.5228 GHz	f_r= 0.5431 GHz
1.0112	1.0225	1.0427
1.5109	1.5221	1.5424
2.0106	2.0218	2.0421
2.5102	2.5214	2.5417
...	...	...

Further analysis on IDs

Occasional jumps in the mode spectrum with ID gap

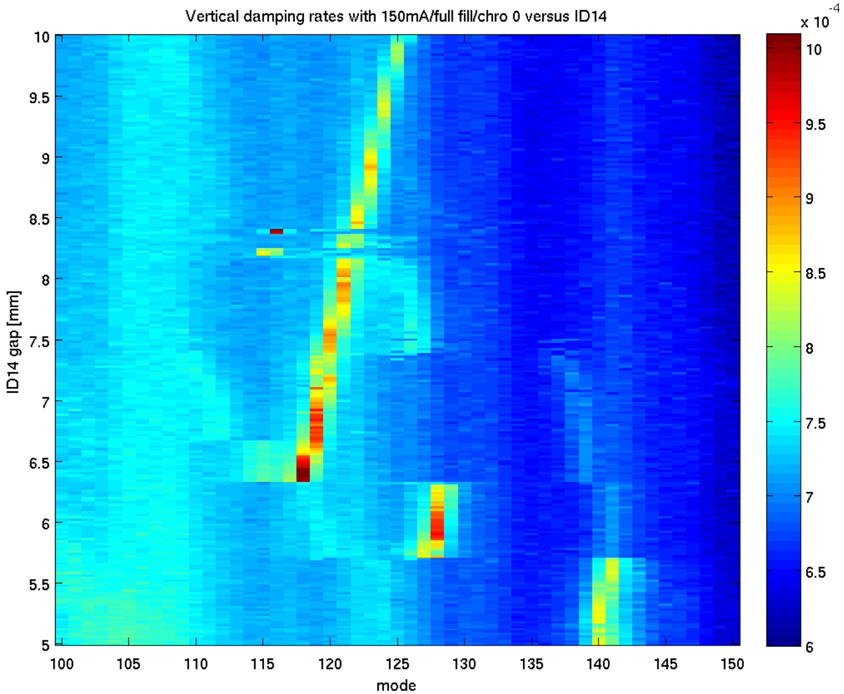

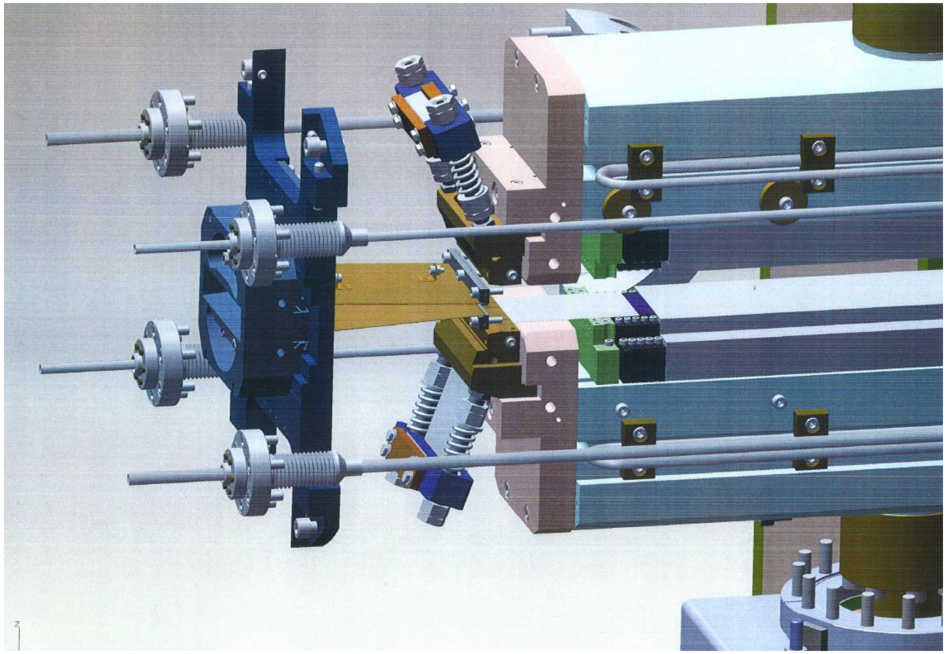

These are however “better understood” as they are clearly correlated to the ID gap changes – jumps of 10 or more modes !

Other measurements (WIP)

Using the functionality of the TMBF, grow damp measurement can be made on many machine configurations repeatedly with time

Different RF voltage
i.e. different bunch lengths

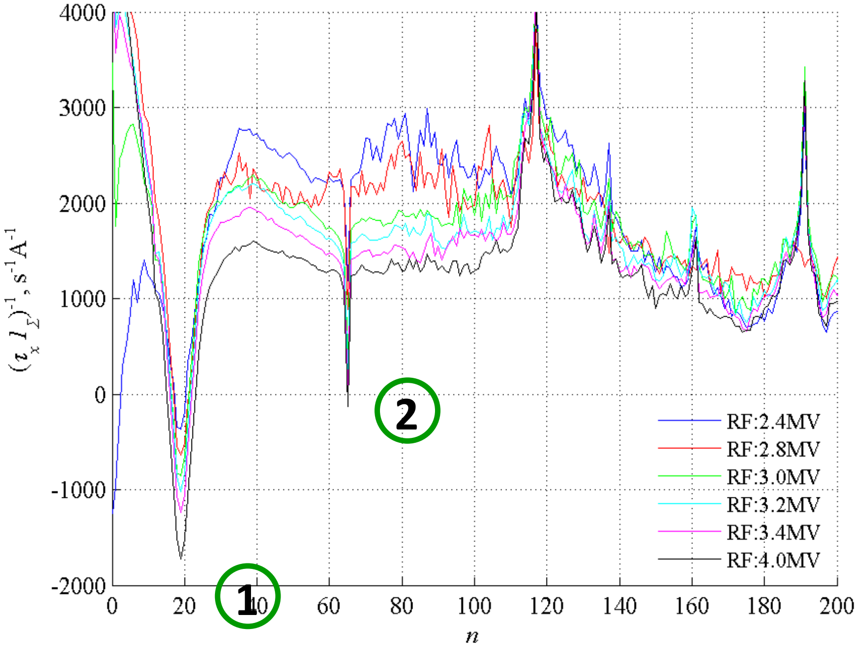

Different chromaticities
i.e. different chromatic damping

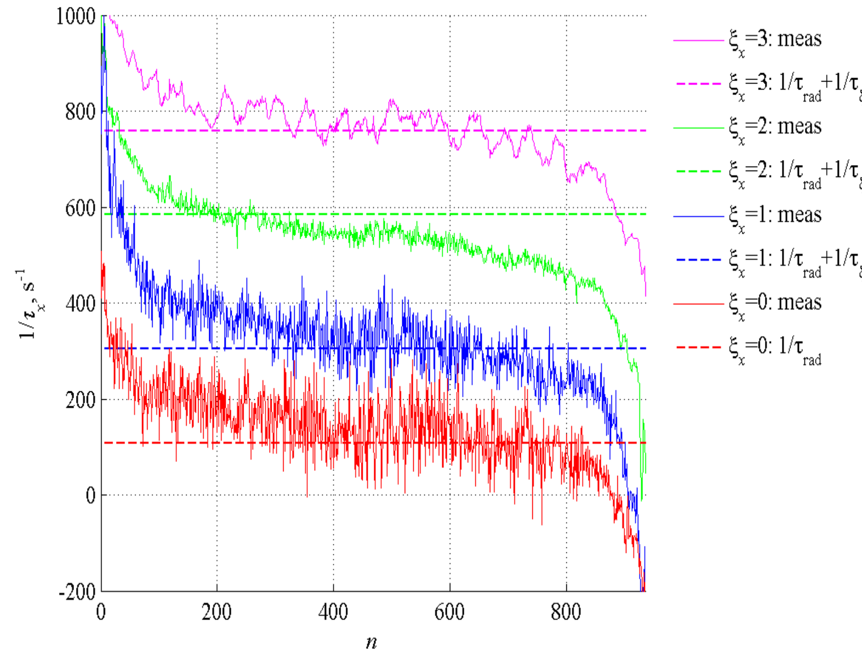

Open issues and conclusions

The Diamond TMBF allowed extensive and repetitive grow damp measurements allowing parameter scan and a regular monitoring of the impedance of the machine

These studies have produced rather surprising results and questioned previous impedance calculations

Although all coupled bunch modes are eventually stabilised by the TMBF system, it is clear that the machine impedance is complicated and changing with time in way that are difficult to interpret and predict.

The specific resonances at Diamond will be further investigated to identify possible causes: IDs, BPMs, RF cavities, Collimators, ...
More quantitative evaluation of the impedance – beyond the qualitative identification of the frequency excited in the spectrum – is forthcoming